ELSEVIER Solar Energy Materials and Solar Cells 41/42 (1996) 87–99

Solar Energy Materials and Solar Cells

24% Efficient perl silicon solar cell: Recent improvements in high efficiency silicon cell research

Jianhua Zhao, Aihua Wang, Pietro P. Altermatt, Stuart R. Wenham, Martin A. Green

Centre for Photovoltaic Devices and Systems, University of New South Wales, Sydney, NSW 2052, Australia

Abstract

Recent research upon high efficiency passivated emitter, rear locally-diffused (PERL) cells has resulted in a considerable improvement in the energy conversion efficiencies of silicon solar cells up to 24.0% under the standard global solar spectrum. Under monochromatic light, energy conversion efficiency of 46.3% for 1.04 μm wavelength light has been measured. These efficiencies are the highest ever reported for a silicon device.

This progress has been achieved by a combination of several mechanisms. One is the reduction of recombination at the cell front surface by improved passivation of the silicon/silicon dioxide interface. Resistive losses in the cell have been reduced by a double-plating process which increases the thickness for the coarse cell metallization features. The reflective losses have been reduced by the application of a double layer anti-reflection (DLAR) coating. Another advantage of DLAR coating is that it will give an additional 3% higher current density than SiO_2 single layer anti-reflection (SLAR) coated cells when encapsulated into modules. Earlier modifications in the cell mask design have also contributed to this improvement, and will also be discussed in this paper.

1. Introduction

The last decade has produced substantial improvements in silicon solar cell performance. As shown in Fig. 1, standardisation of past measurements has shown there has been a 42% improvement in the highest independently confirmed efficiency between 1983 and 1990 [1]. This improvement was proceeded by substantial improvements in the open-circuit voltage of experimental devices. Since the open-circuit voltage depends

SSDI 0927-0248(95)00117-4

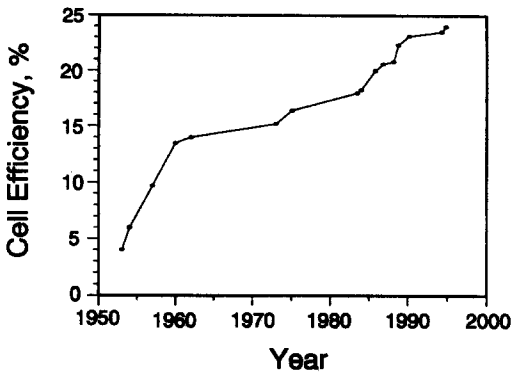

Fig. 1. Progress in Laboratory silicon solar cell efficiency.

logarithmically on recombination within the active areas of the cells, a small improvement in open-circuit voltage corresponds to a large improvement in device quality.

Research on the passivated emitter cell series (PESC, PERC and PERL) at the University of New South Wales (UNSW) has made a major contribution towards this improvement [1]. Recent research at UNSW has resulted in further significant improvement in the cell efficiencies up to 24%.

The latest cell structure developed at UNSW is the passivated emitter, rear locally-diffused (PERL) cell. The PERL cell demonstrated an energy conversion efficiency of 23.1% in 1990 [2,3]. One of the major advantages of PERL cells over conventional silicon cells is the improved surface passivation demonstrated by a thermally grown oxide in the trichloroethane (TCA) ambient [2]. This improved surface passivation significantly reduced the emitter saturation current density and hence improved the cell open-circuit voltage to above the 700-mV level. This oxide also serves as a SLAR coating, although it causes about 3% reflection loss at the cell front surface.

2. New PERL cell design

The PERL cells had been redesigned in 1993 with the cell structure shown in Fig. 2. Beside the TCA oxide passivation of the cell front and rear surfaces, the front and rear contact areas are also passivated by heavily diffused phosphorus and boron areas, respectively. Hence, the recombination at these contact areas has also been significantly reduced due to the suppressed minority concentration in the areas. The boron diffused rear contact passivation allows 250-μm spacing for the 10 μm by 10 μm rear contacts to achieve low series resistance for the device. Boron tribromide (BBr_3) liquid source diffusion is used for this rear contact passivition due to the low surface damages attributed to this method.

The new PERL design also has following features different from the previous design [4]:

(a) The metal shading loss have been carefully reduced from 4% of the previous design to 3.5%. The front contact line width has also been reduced from the earlier value

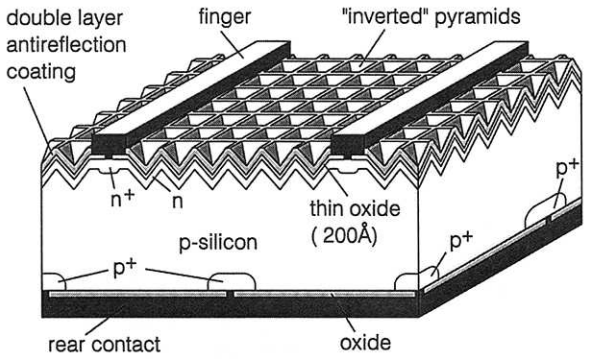

Fig. 2. Passivated emitter, rear locally-diffused (PERL) cell with a double layer anti-reflection coating.

of 2.5 μm to 2 μm. The reduced contact areas reduce the total recombination at the contact. This may contribute to higher open-circuit voltage in the device. The design also further reduced the emitter contact areas using a dotted contact structure, even though the improvement due to this method was considered insignificant.

(b) The emitter area of the cell has been well defined by using an aluminium aperture mask. This eliminated the possible test errors which occurred during measurement when an aperture mask was placed on top of the wafer to shade the cell peripheral area and to define the test cell area. The aluminium layer introduced to the cell front surface can be also used to perform an "alneal" process, which will be discussed later.

(c) The spacing between cells on the same wafer has been increased to 5 mm, from 0.7 mm in the previous design. The coupling between cells could result in lower measured cell performance since the neighbouring cell was always shaded during the measurement. The increased spacing reduced this coupling effect, even though considerable coupling between cells is still observed in the present cells with some consequent loss in measured performance.

(d) 370 or 400-micron thick, 10-cm diameter wafers are processed using improved 10-cm wafer processing facilities [4]. The thicker substrates increase the expected short-circuit current density from the cells. The modified equipment gives better processing repeatability. It also takes advantage of more recent wafer fabrication technology than that used for the earlier 5-cm wafers.

(e) Phosphorus tribromide (PBr_3) has been used as diffusion source for both emitter and front contact passivation diffusions. As boron tribromide diffusion could reduce surface damage [2], cells with PBr_3 diffusion also demonstrated higher open-circuit voltages than obtained with the previous solid source phosphorus diffusion.

(f) Different spacing between the front metal fingers is also incorporated into the cell design due to recent results of numerical analysis [5]. This analysis showed a reduced effective emitter lateral resistance due to the electron lateral movement in the bulk region as well as in the emitter [5]. Finger spacing of 500 μm, 800 μm and 1110 μm have been chosen in the design.

(g) Different sized cells are also designed to examine the size effect upon the cells. Cell areas of 1 cm × 1 cm, 2 cm × 2 cm, and 2 cm × 4 cm are included in the design.

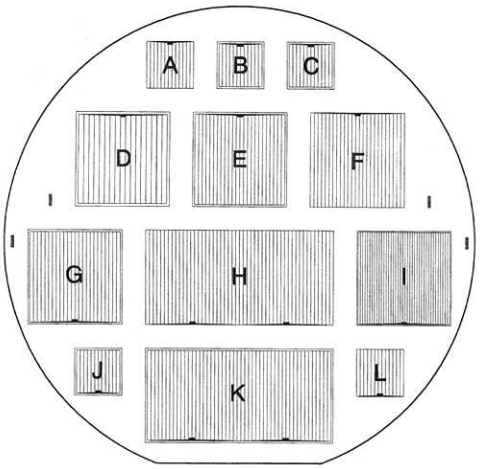

Fig. 3. The cell layout on a 10-cm wafer for the new PERL cell design.

The layout of the cells on a 10-cm wafer with all the above mentioned features is shown in Fig. 3. A total of 6 to 8 photo masking steps are required for the cell processing depending on which features are chosen. Since the aim of this research is to find the highest possible efficiency which a silicon cell can achieve, the processing complexity and the cost in fabricating these cells were not issues for this research.

3. Initial experiment with the new design

The modified PERL cell initially demonstrated an improved efficiency of 23.5% [4]. Some of the newly designed features contributed considerably to the cell performance improvement while some others did not. This section mainly discusses a few interesting effects encountered in the new design.

3.1. Dotted emitter contact

The dotted emitter contact was designed to further reduce the recombination at the emitter contact area. However, an extra masking step is required to open the contact area. A double exposure masking process is used to open the dotted contact, then the metal pattern. However, the process was found sometimes to cause series problems for the final metallisation.

A slight improvement in the open-circuit voltage was found, restricted to a couple of millivolts. It is believed that the recombination at the metal contact areas in the PERL cells is not dominant due to the double diffusion passivation. The dotted emitter method was also found not compatible with the thin oxide DLAR cells. Hence, the dotted emitter contact design was discarded after the initial stages of the experiments.

3.2. Coupling between the cells

Even though the spacing between the cells has been increased to 5 mm, considerable coupling between the cells has been observed. A considerable amount of minority carriers can diffuse through this 5 mm distance to reach the neighbouring cells due to the extremely long minority carrier diffusion length in these PERL cells. Another experiment with a MOS structure between the cells showed that there was no strong inversion layer at the silicon surface between the cells. Hence, there is little possibility for minority carriers coupling through such surface channels.

In the normal cell testing, all the cells except the one being measured are shaded by an aperture mask. When the neighbouring cells are exposed in the measurement, the measured short-circuit current density has shown an increase from 4 to 7 mA for the 4 cm^2 cells on 1.0 Ω-cm substrates. Table 1 shows a result from a few typical cells for such measurements. More research is needed to further reduce this coupling effect.

3.3. Different spacing between the front metal fingers

For a lightly doped emitter of about 150 Ω/□ for PERL cells on 1 Ω-cm substrates, it was expected that larger finger spacing could improve the cell open-circuit voltages with little reduction on the cell fill factors, based on the 2-D analysis results [5]. The cells with 1110 μm finger spacing demonstrated an average 2-mV higher open-circuit voltage than 800 μm spacing cells. However, they suffered considerable loss in the fill factors. Hence, their efficiencies were always lower than 800 μm spacing cells.

On the other hand, the cells with 500 μm spacing suffered a considerably lower open-circuit voltages with little change in their fill factors. Hence, the optimum is the same spacing as the earlier PERL cells of 800 μm.

3.4. Different cell sizes

It was expected that the metal resistance loss can be considerably reduced for the smaller cells. However, in the 1 cm^2 cells, the increase in the fill factors is overwhelmed by the reduction in the cell short-circuit current densities attributed to effects from the cell periphery. For the lager 8 cm^2 cells, for some, as yet, unexplained reason, the cells

Table 1
The performance of the new PERL cell design when all the cells on the wafer are illuminated compared to the case when only the measured cell is illuminated. The large current differences from the two conditions show a strong interaction between cells (cell area is 4 cm^2)

Cell no	Illumination	V_{oc} (mV)	I_{sc} (mA)	FF (%)	E_{ff} (%)
W4-1-4-9	one cell	701	161.6	81.1	23.0
W4-1-4-9	all cells	702	166.8	81.1	–
W4-1-2-9	one cell	698	162.0	80.8	22.8
W4-1-2-9	all cells	700	166.0	80.9	–

always give a little lower values of J_{sc}, V_{oc} and FF. Hence, the 4 cm^2 cells always give the best result.

4. Atomic hydrogen passivation: "alneal" process

A recent development has been to apply a DLAR coating to the PERL cells to further reduce their surface reflection loss, as shown in Fig. 2. To achieve low surface reflection, the thickness of the thermally grown oxide underneath the coating layers has to be reduced to below 300Å [6]. The earlier difficulties in the application of these DLAR coatings was due to the reduced surface passivation performance when the thickness of thermal-grown oxide was reduced. The present work employed atomic hydrogen passivation, which has given significantly improved surface passivation especially for these thin passivation oxides.

In the present work, passivation oxides with different thicknesses are grown in TCA ambient, then annealed in forming gas. Table 2 compares the performance of these cells. The lower voltages of the cells with thinner oxides result from the poorer surface passivation quality of these oxides. An earlier attempt to etch thick oxides back to the required thickness for DLAR coating was only partially successful, attributed to non-uniform etching on a microscopic scale [7].

The solution was found by atomic hydrogen passivation of directly-grown thin oxides. The atomic hydrogen passivation is realised by the so-called "alneal" (aluminium anneal) process [8,9]. In this process, a layer of aluminium is evaporated onto the cell front surface. The cells are then annealed in forming gas at about 370°C for 30 min. The aluminium on the cell active areas is then etched off in phosphoric acid. The rest of the aluminium around the cell periphery is protected by photoresist and left on to act as an aperture mask to accurately define the cell area. During the annealing step, it is believed that the aluminium reacts with hydroxyl ions within the oxide to generate atomic hydrogen. The atomic hydrogen then migrates to the Si/SiO_2 interface and passivates defects such as dangling bounds. Repeating the experiment of Table 2 with this "alneal" processing improvement produced devices with improved open-circuit voltage of close to 709 mV after application of DLAR coating regardless of oxide thickness over the range shown. This is about 7 mV higher than the best earlier PERL cells without this feature [4].

Table 2
The performance of PERL cells with different oxide thicknesses. The oxide has been grown in a TCA ambient and annealed in forming gas

Cell ID	Oxide thickness (Å)	J_{sc} (mA/cm^2)	V_{oc} (mV)
W4-19-2E	200	36.5	682
Z4-16-2E	600	37.5	697
W4-6-1H	1100	40.7	703

Table 3
The measured effective minority carrier lifetimes at different processing stages for an 1.5 Ω-cm FZ wafer with 1100Å TCA grown oxide. "Alneal" and forming gas anneal significantly improved the carrier lifetimes

Processing stage	τ
After TCA oxidation	14 μs
After sinter in forming gas	40 μs
After "alneal"	400 μs

The "alnealing" step was automatically included in earlier processing of the rear surface, since aluminium is used as the rear contact metal. The "alnealing" which occurs at peripheral areas of the top surface is also thought very important, since these peripheral areas are not doped. Surface recombination can be also much higher in these non-illuminated areas exacerbating the reduction in current and voltage output caused by these regions [10].

The surface passivation effect of forming gas anneal and "alneal" is also examined with an 1.5 Ω-cm double side polished wafer with 1100Å-thick TCA grown oxide. A Leo Giken lifetime tester is used to test the carrier lifetimes in the wafers. The test results are shown in Table 3. The effective minority carrier lifetime is measured as 14 μs directly after oxide growth. The carrier lifetime then increases to about 40 μs after annealing in forming gas with 4% hydrogen component. Hence, the forming gas anneal is critical for the PERL cell processing [2]. However, more significant improvement is found in the "alneal" process, which increased the effective carrier lifetime up to 400 μs.

Due to the improved surface passivation effect from the "alnealing" process, many earlier experimental conclusions require re-evaluation, such as those for the thin cells and for the dotted emitter cells. Since, these cells did not use the "alneal" process, the experimental modifications could not improve the cell performance possibly due to the relatively higher surface recombination component. However, the situation may be different if an "alneal" is incorporated into these experiments in the future.

5. Double layer antireflection (DLAR) coating

A ZnS and MgF_2 DLAR coating is evaporated onto the cells processed with the "alnealed" thin oxide. Fig. 4 shows the reflection, external and internal quantum efficiencies of such a cell. The DLAR coated cell has over 2.5% lower weighted reflection than the earlier single layer SiO_2 coated PERL cells. In the medium and long wavelength range, the internal quantum efficiency of the DLAR coated cell is similar to the earlier single layer coated cell. However, due to the wider external response, the double layer coated cell has a considerably improved external response over the range from 0.8 to 1.1 micron wavelength. Below 0.4 micron wavelength, the absorption in ZnS layer reduced the cell response. Further experimentation with different materials will possibly reduce this loss.

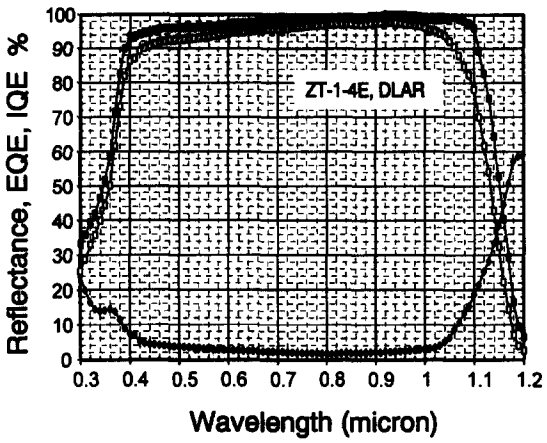

Fig. 4. Front surface reflection, external and internal quantum efficiencies of a PERL cell with a double layer antireflection coating.

Between 0.4 and 0.8 micron wavelength, the cell internal response reduced considerably below unity. It is still not sure that if this is due to a surface damage during the coating material application or an excessively heavily diffused emitter region. More work is needed to identify the reason for this effect and to minimise it.

Another important advantage of the PERL cell with DLAR coating over the earlier PERL cells with SLAR SiO_2 coating is that they will have 3% lower reflection when encapsulated. The SiO_2 SLAR virtually loses its anti-reflection property when encapsulated, due to the similar refractive indices of EVA encapsulation and of SiO_2. In spite of this loss, a solar cell module with SiO_2 SLAR coated PERL cells demonstrated 20.6% efficiency [11] (since revised to 20.8%). It is expected that with the DLAR coated PERL cells and other recent improvements, it is now possible to achieve over 22% module efficiency. A project is now planned to fabricate such modules in the near future.

6. Reduced metal resistance loss

Relatively low fill factors had been another limiting factor for the PERL cells in the past [10]. Voltage dependence of the rear surface recombination velocity was thought a major contributor to this effect [10]. However, careful measurement of cell losses, excluding non-linear effects due to the previous mechanism, showed significant Joule resistive loss [12]. Cell series resistance was measured as 0.5 Ω-cm^2, with a contribution from the front metal grid of 0.3 Ω-cm^2 [12].

The plating process used to increase the metallization grid conductivity also broadens these metallization features as it increases their thickness. Since the cells are illuminated in the plating solution, the lower densities of light-generated current near coarse features result in less metal plating in these areas. This was producing excessive voltage drop along coarse features, such as the cell busbar. This is demonstrated by Fig. 5a, which

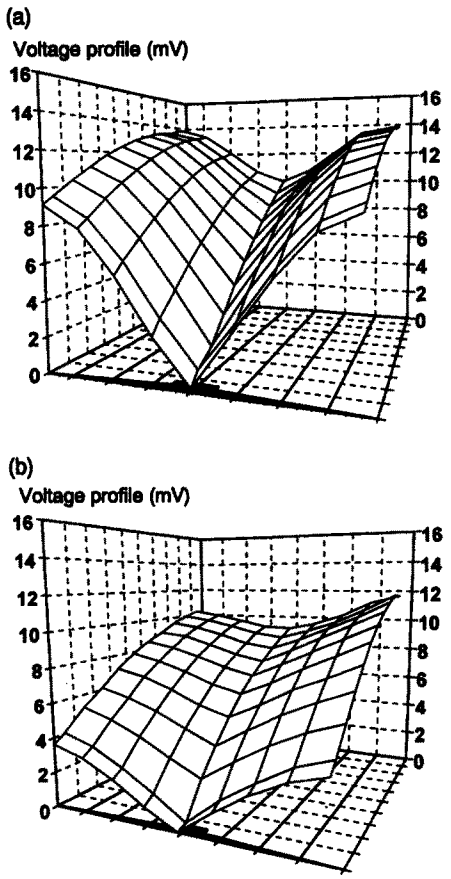

Fig. 5. The measured voltage distribution over the metal grid for a 4 cm^2 cell at the maximum power point of: (a) an earlier PERL cell (cell W413E); (b) a cell with double busbar metal plating (cell ZT-1-1E). The voltage drop along the grid is significantly reduced in case (b).

shows the measured voltage distribution along the cell metallization for a 4 cm^2 cell at the maximum power point (not all the metallization fingers are shown). The cell busbar caused more voltage drop than the fingers even though their length is only half that of fingers. In spite of the large voltage drop along the metal grid, the particular cell has a fill factor of 81.2%, which is a relatively high fill factor for the earlier PERL cells.

A two step metal plating sequence was developed to correct for this deficiency. AZ4620 photoresist is used to protect most of the fine metallization fingers during the second plating step, where the coarse busbar is further plated. This has significantly reduced Joule resistive losses as shown by the voltage profile of Fig. 5b. The total series resistance of the cell is reduced to 0.3 Ω-cm^2 in this way. Hence, the cells demonstrated fill factors higher then 83%. This is the first time for a 4 cm^2 PERL cell to demonstrate such a high fill factor.

7. Cell performance

7.1. Improved cell dark I–V curve

A considerable improvement in the cell dark I–V curves have been observed from the "alneal" processed cells than the earlier single layer SiO_2 coated cells. This is shown in Fig. 6. The "alnealed" cell (ZT-1-1E) kept the similar three-section shape of the I–V curve as the earlier PERL cell (Wb124-L). The three section performance is a result of the rear surface recombination changing with bias [10]. However, the "alnealed" cell has this section of the curve shifted to a lower bias range. This may be an effect of the reduced surface recombination. This shift reduces its detrimental effect upon the cell fill factors. Hence, higher than normal fill factors of around 81.8% were demonstrated for these cells even before the secondary metal plating.

7.2. Improved AM1.5 efficiency of 24.0%

Cells with 200Å oxide and MgF_2/ZnS DLAR coatings were processed with these improvements on 1.0 and 1.5 Ω-cm float zone substrates and independently tested at Sandia National Laboratories. The results are shown in Table 4. Two cells fabricated both on 1.0 and 1.5 Ω-cm substrates demonstrated efficiencies of 24.0% under the global AM1.5 spectrum (100 mW/cm^2) at 25°C (aperture area basis [3]). These are the highest conversion efficiencies ever reported for a silicon cell.

The main improvements over earlier devices [1,3] are in open-circuit voltage and fill factor due to the "alnealing" and 2-step plating processes, as previously explained. Current output was slightly lower than possible, probably due to a marginally non-optimal top surface diffusion. The ZnS layer in the DLAR coating also becomes strongly absorbing at wavelengths below 0.39 μm, reducing current density by between 0.5–1.0

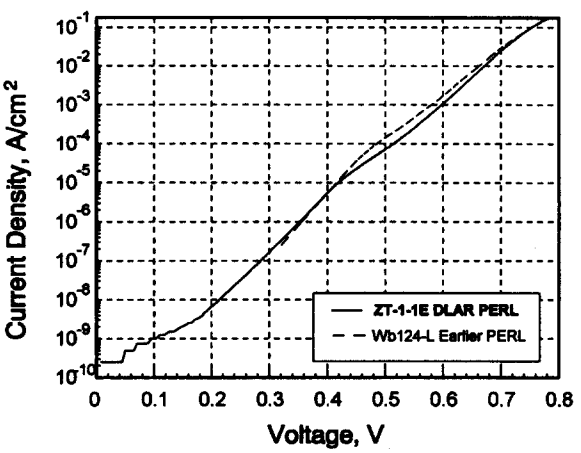

Fig. 6. The measured dark I–V curve of a DLAR coated PERL cell (ZT-1-1E). The dark I–V curve of an earlier PERL cell (Wb124-L) is also shown.

Table 4
Output parameters of high-performance 4-cm^2 PERL silicon solar cells as measured by Sandia National Laboratories, under the global AM1.5 spectrum (100 mW/cm^2) at 25°C

Cell ID	ρ_b (Ω-cm)	V_{oc} (mV)	J_{sc} (mA/cm^2)	FF (%)	Effic. (%)
ZT-1-3E	1.0	707	40.7	83.0	23.9
ZT-1-4E	1.5	708	40.8	83.1	24.0
ZT-1-5E	1.0	709	40.9	82.7	24.0

mA/cm^2. Further improvements seem likely to produce cell efficiency above 25% by further optimization of the emitter doping profile and using other less absorptive coating materials than ZnS.

Thinning the substrate may also improve the cell voltage. The earlier non-optimal performance from thin PERL cells may have been a result of high recombination at the front surface. The alneal process may be a powerful tool to further improve the cell V_{oc}, without appreciable loss in J_{sc} for the thin cells.

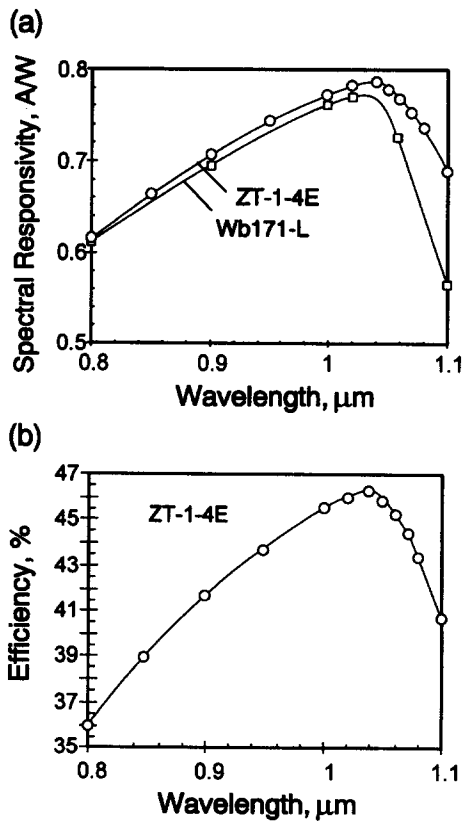

Fig. 7. (a) Wavelength spectral response of a present DLAR PERL cell ZT-1-4E, and the best earlier SLAR PERL cell Wb171-L. (b) Conversion efficiency of the DLAR PERL cell ZT-1-4E.

7.3. Improved long wavelength responsivity of 0.787 A / W and monochromatic light efficiency of 46.3%

Earlier PERL cells have demonstrated 45.1% efficiency under 1.02 μm monochromatic light [13]. The low recombination at the surface and in the bulk region, and the excellent light trapping scheme using inverted pyramids and a rear aluminium mirror have contributed to this performance [14]. The DLAR coated PERL cells demonstrated a further improved external response and conversion efficiency under long-wavelength monochromatic light. The DLAR coated cell has a responsivity of 0.787 A/W independently measured at Sandia National Laboratories at a wavelength of 1.04 μm. Fig. 7a shows the long-wavelength spectral response of the cell. For comparison, the best previous PERL cell with SiO_2 SLAR coating is also plotted in the figure. The DLAR coated cell has a considerably higher response especially at the very long wavelength range. Fig. 7b shows the efficiency of the DLAR coated cell. It demonstrated a record conversion efficiency of 46.3% for light of 1.04 μm wavelength at an incident light intensity of 51.8 mW/cm^2.

8. Conclusion

Silicon solar cells with 24.0% conversion efficiency have been reported. The cells also demonstrated an record efficiency of 46.3% and a responsivity of 0.787 A/W under 1.04 μm monochromatic light. The new cell mask design, atomic hydrogen passivation, a DLAR coating, and an increased thickness of coarse cell metallization features have contributed to these improved results. Silicon cell efficiency of 25%, therefore, appears attainable in the near future. The DLAR coating also has a better matching factor for module encapsulation. This will enhance the application possibilities for these cells.

Acknowledgements

The authors would like to thank Yinghui Tang, Ximing Dai, Armin G. Aberle, Mark Silver, and other members of the Centre for Photovoltaic Devices and Systems for their contribution to this work. The contributions of Paul Basore and colleagues at Sandia National Laboratories in the area of cell characterisation are gratefully acknowledged. This work is partially supported by the Australian Research Council and the Energy Research and Development Corporation. The Centre for Photovoltaic Devices and Systems is supported by the Australian Research Council's Special Research Centre Scheme and by Pacific Power.

References

[1] M.A. Green, in: Proc. 10th EC Photovoltaic Solar Energy Conf., Lisbon (Kluwer, Dordrecht, 1991) p. 250.

[2] A. Wang, J. Zhao and M.A. Green, Appl. Phys. Lett. 57 (1990) 602.
[3] M.A. Green and K. Emery, Progr. Photovolt. 2 (1994) 27.
[4] J. Zhao, A. Wang and M.A. Green, Progr. Photovolt. 2 (1994) 227.
[5] A.G. Aberle, S.R. Wenham, M.A. Green and G. Heiser, Progr. Photovolt. 2 (1994) 3.
[6] J. Zhao and M.A. Green, IEEE Trans. Electron Dev. ED-38 (1991) 1925.
[7] J. Zhao, A. Wang and M.A. Green, IEEE Trans. Electron Dev. ED-41 (1994) 1592.
[8] P. Balk, The Si-SiO_2 System (Elsevier, Amsterdam, 1988) p. 234.
[9] R.R. King, R.A. Sinton and R.M. Swanson, IEEE Trans. Electron Dev. ED-37 (1990) 365.
[10] A.G. Aberle, S.J. Robinson, A. Wang, J. Zhao, S.R. Wenham and M.A. Green, Progr. Photovolt. 1 (1993) 133.
[11] J. Zhao, A. Wang, M. Taouk, S.R. Wenham, M.A. Green and D.L. King, IEEE Electron Dev. Lett. 14 (1993) 539.
[12] P.P. Altermatt, Two-dimensional Numerical Modeling of High-efficiency Silicon Solar Cells, Diploma Thesis, University of New South Wales (1994).
[13] M.A. Green, J. Zhao, A. Wang and S.R. Wenham, IEEE Electron Dev. Lett. 13 (1992) 317.
[14] M.A. Green, Surface Texturing and Patterning in Solar Cells, in: M. Prince (Ed.), Advances in Solar Energy, Vol. 8 (American Solar Energy Society, Boulder, 1993) pp. 231–269.